An Accurate Fault Location on Mutually Coupled Transmission Lines Using Synchronized Sampling

B. Perunicic, A.Y. Jakwani
Lamar University, Beaumont,
Texas, USA

M. Kezunovic
Texas A&M University, College Station

Abstract - The mutual inductance between parallel transmission lines influences the locating of the transmission line faults. A fault location algorithm for parallel lines developed in this paper takes into account the magnetic coupling between parallel lines. The paper presents a detailed description of the developed algorithm and test results performed on a simplified real transmission line. The obtained error is less than 0.5 percent in most cases. Also, the developed algorithm is not sensitive to typical fault parameters, such as: resistance, type, location, and incidence angle.

INTRODUCTION

In urban and industrially dense regions with a high consumption of electrical power, transmission lines are placed in parallel, often on the same tower. Due to a high mutual inductance, a current in one line induces voltage in the nearby line. As a result, current in one line depends on the current in the parallel line. If the fault location algorithm does not account for the induced voltage due to the magnetic coupling, the outcome of algorithm may be erroneous. However, it was impossible to successfully account for the mutual inductance between parallel lines until the synchronized samples of voltages and currents of both lines were considered. It is just recently that the hardware to support this need (GPS, optical communication links, satellite beacons etc.) have become available at a reasonable cost [1-3].

The aim of this paper is to develop a new algorithm that will take into account the influence of the mutual inductance. First, it is shown that the mutual inductance between parallel lines introduces a significant error in the location of the fault. An accurate time-domain fault location algorithm [4-5] is used to determine the influence of the magnetic coupling on the fault location. Then, a new algorithm is presented to account for the voltage induced due to the parallel line. It is assumed that synchronized samples of voltages and currents of two parallel lines have been taken during the transient, post-faulted state, for example, by using a digital fault recorder (DFR) with GPS receivers [3], and communicating the data to the DFR at the other end of the line. Based on these samples, the algorithm estimates the induced voltage in the faulted line due to the current in the nearby parallel unfaulted line. The algorithm does not involve any other approximation, nor preprocessing of the data samples. The test results show that the algorithm is not sensitive to the typical fault parameters, such as: resistance, type, location, and incidence angle.

FAULT LOCATION TECHNIQUE

General Concept

The algorithm presented in this paper is an extension of the approach presented in papers[4] and [5]. The paper [4] describes an algorithm suitable for a short transmission line, while the paper [5] introduces an algorithm for a long transmission line. It is assumed that samples of voltages and currents, synchronously taken after the fault, are available for the fault location calculations. The algorithms presented in these papers are very accurate and have a low sensitivity to the typical fault parameters, such as, resistance, type, location, and incidence angle. Moreover, the resistance of the fault may change during the fault. The algorithm is capable of calculating the location of the arcing type of the fault.

Since the lines in industrialized areas where the mutual inductance effects are likely to occur are relatively short, the short transmission line model is considered in this paper. The original algorithm in [4] uses a single homogenous line generic model. Based on this approach, a new model for parallel lines is derived. The algorithm obtained from this model uses voltage and current samples in the faulted line and samples of the current in the parallel unfaulted line. This algorithm was tested using model of a

real transmission line in Beaumont, Texas. Since this line is not a homogenous one, the model was simplified for the preliminary testing purposes. As a next step, the authors intent to derive a new algorithm suitable for non-homogeneous parallel lines, and then test the algorithm on the model of an actual line.

Model of the Parallel Transmission Lines

The sketch of the parallel lines used in this project is shown in Fig. 1. The two lines have a common sending end (S) and are parallel along a portion of the their entire length. The fault may occur in the part where the two lines share a tower, or in the part where there is only one line on the tower. The presence of the other line on the tower influences the parameters of the transmission line. In the shared part of the line the parameters resistance [r] and inductance [l] are indicated by the superscript (') and in the rest of the line they are the same as for the single line. It will be shown in the following sections that fault location calculations for parallel lines can be reduced to the single line fault location calculations.

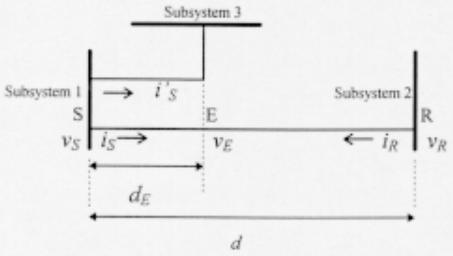

S - sending end; R - receiving end

Fig 1. Three Phase Non-Homogeneous, Unfaulted Power System

First, assume that the fault is in the parallel part of the non-homogeneous line (Assumption 1, see Fig. 2). The voltages and currents represented in this figure are the vectors of three-phase quantities. The part of the line between the points E and R is homogenous and unfaulted. Therefore, the voltage v_E at the place E where the two lines separate may be calculated using the receiving end voltage v_R, and the receiving end current i_R as given in [4] (see Appendix A).

$$v_{Em}(t)=v_{Rm}(t) -(d-d_E) \sum_p [r_{mp}\, i_{pR}(t) + l_{mp}\, di_{pR}(t)/dt] \quad \ldots\ldots(1)$$

p = phases a, b, c
m = phases a, b, c
r_{mp} and l_{mp} are single line parameters.

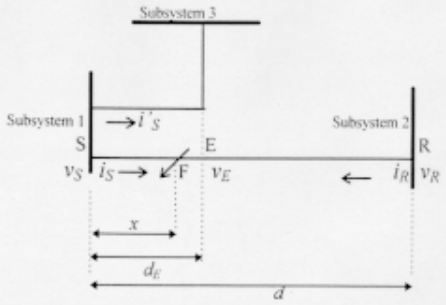

Fig 2. Fault in the Shared Part of the Power System (Assumption 1)

The line between the points S and E is a homogenous parallel line, and the voltage v_E is given by equation (1). The current i_E is obviously equal to the current i_R. The model of the line between S and E differs from the single line model derived in [4] because the currents i'_S in the parallel line induce the voltage v_M in the faulted line. The induced voltage v_M is defined by the equation:

$$v_{Mm}(t) = d_E \sum_{p'} [r_{mp'}\, i_{p'}(t) + l_{mp'}\, di_{p'}(t)/dt] \quad \ldots\ldots(2)$$

p' = a', b', c' [Phases in the parallel line]
m = a, b, c

Due to the induced voltage v_M, the voltage difference between the point E and S will be equal to:

$$v_S - v_E + v_M = v_S - (v_E - v_M) \quad \ldots\ldots(3)$$

It is obvious that the fault location equation derived for the single line may now be used (see Appendix A for the generic and derived fault location equations), if the voltages v_S and v_R from the single-line algorithm are replaced by:

$$v_S = v_S \quad \ldots\ldots(4)$$
$$v_R = v_E + v_M \quad \ldots\ldots(5)$$

Now, assume that the fault occurred in the non-shared portion of the power line (Assumption 2, see Fig. 3). The voltage v_E in this case is defined by the equation:

$$v_{Em}(t)=v_{Sm}(t)+v_{Mm}-d_E \sum_p [r'_{mp}\, i_{pS}(t)+ l'_{mp}\, di_{pS}(t)/dt] \quad \ldots\ldots(6)$$

p = a, b, c and m = a, b, c

The part of the line between E and R is homogenous, and again the fault location equation for the single line may be used, but the sending end voltage is now equal to V_E, the line length of the line is $(d-d_E)$, and the location of the fault obtained is the distance x from E to the

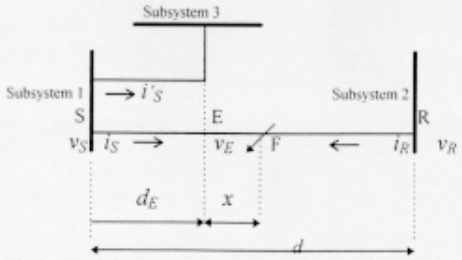

Fig 3. Fault in the Non-Shared Part of the Power System (Assumption 2)

fault. Therefore, voltages v_S and v_R in the single-line location algorithm should be replaced by:

$$v_S = v_E + v_M \quad \text{.....(7)}$$
$$v_R = v_R \quad \text{.....(8)}$$

Description of the Algorithm

The above considerations are the base for the developed algorithm. Since the location of the fault is unknown, the calculation starts with the assumption that the fault is in the shared part of the line (Assumption 1). If the result shows that the location is indeed in this part, the calculation is finished. If this is not the case, it is assumed that the location is in the non- shared part (Assumption 2), and the correct location is determined. The flow diagram of the algorithm is shown in Fig. 4.

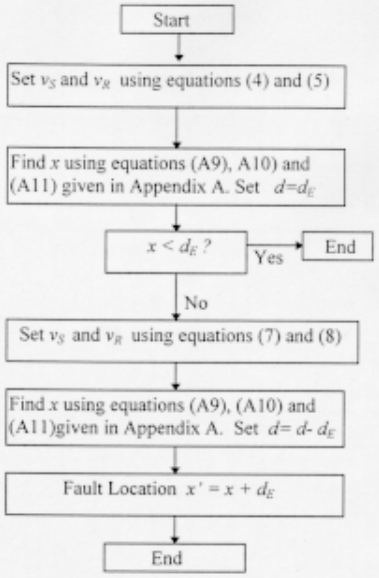

Fig 4. Flow Diagram of the Algorithm

PERFORMANCE EVALUATIONS

Description of the Performed Tests

To determine the performance of the developed algorithm, Electromagnetic Transient Program (EMTP) was used to simulate the power system of Fig. 1 [6,7]. The model was a 138kV power transmission line. The length of the shared part was 0.7 miles, whereas the total length of the transmission system was 1.6 miles. The parameters of the single transmission line, and the parallel transmission lines line are obtained using the EMTP auxiliary routine AUX. The total time of the simulation in the test runs was T_{tot} = 50.0msec, while the sampling time step was Δt = 200.0μs. Four types of faults, line to ground, three phase fault, line to line fault and double line to ground fault, are simulated to determine the performance of the algorithms. The test cases were generated by varying the four parameters of the fault event. These parameters are:

a. Fault location
b. Fault resistance
c. Type of the fault
d. Incidence angle of the fault occurrence

These four parameters are varied between their upper and lower boundaries to enable the extensive coverage of possible real events. The considered locations of the fault were 0.25, 0.45, and 0.75, where 1.0 is the entire length of the transmission line. The fault resistance values were R_f = 3Ω and R_f = 30Ω. The incidence angles of zero and ninety degrees are simulated with all four types of faults to test the performance of the algorithm.

Results

For comparison, all simulated fault locations are first calculated using the single line algorithm of [4] (Tables I, III, V, VII). Then, the new algorithm for parallel lines developed in this paper is used to compute the fault location using assumptions one and two (Tables II, IV, VI, VIII-XII). For different fault-event parameters described in the previous section, the error in fault location algorithms was calculated. The error in percentage of the fault location is defined by:

$$\text{error} = \frac{|\text{actual fault loc.} - \text{calculated fault loc.}|}{\text{total line length}} * 100\%$$

In all the test cases, assumption that the fault is in the shared portion of the transmission line is considered first. If the calculated length was less than the length of the shared portion, then the outcome is taken as the result. Otherwise, assumption two is applied. Consequently, first assumption was applied to calculate the fault location using both single line and parallel line algorithms (Tables I-VIII). It can be seen that for fault location of 0.75, that is when fault is in the non-shared part of the line, the first assumption does not give accurate results. Application of the second assumption for fault location greater than 0.45 yielded accurate results (Tables IX-XII). For second assumption, fault location calculations for 0.25, and 0.45 are not needed, as they are already determined under first assumption.

Comparing the results of single line and parallel line algorithm, it can be seen that the mutual inductance between parallel lines significantly influences the calculation of the location of the fault. It can be observed that calculation for the single line to ground fault is significantly influenced by mutual inductance, the average error is 3.90 percent while the largest error is 8.50 percent (Table I). The calculation for the three other types of faults are not drastically influenced by mutual inductance, the average error is 0.8 percent (Tables III, V, VII), while the largest error is 9.1 percent (Table V). One should keep in mind that single line to ground fault is most likely to occur under abnormal circumstances.

The parallel line algorithm, developed in this paper, successfully reduces the error in the fault location. In most cases, the average error is 0.50 percent (II, IV, VI, VIII-XII). Also, it can be seen that in most cases, the algorithm is only slightly affected by other fault-event parameters, such as, fault resistance, incidence angle, and location of the fault. However, the algorithm does not provide accurate results under all condition. For example, in Table II for fault location 0.25, R_f = 30 Ω, and incidence angle = 90°, the algorithm gives an error close to two percent. Similarly, In Tables VI, for R_f = 30Ω, with incidence angle of 0°, and fault location of 0.25 and 0.45, and in Table XI, for R_f = 30Ω, incidence angle 0°, and fault location of 0.75, algorithm gives a very high error. Except these four stated cases of fault events, the error in the rest of the fault-event cases is very low. For a wide range of cases, the error is of the order of 0.1 percent, and less than 0.5 percent in most of the cases.

Table I. Error in % using Single-Line Algorithm

Simulation Parameters	Phase A to Ground Fault					
Fault Location	0.25		0.45		0.75	
Incidence Angle	0 deg	90 deg	0 deg	90 deg	0 deg	90 deg
Rf=3Ω	4.5509	4.7877	7.8966	8.4706	0.9834	0.7856
Rf=30Ω	0.6245	2.1700	4.4688	7.8678	2.6632	1.4753

Table II. Error in % using Parallel-Line Algorithm (Assumption 1)

Simulation Parameters	Phase A to Ground Fault					
Fault Location	0.25		0.45		0.75	
Incidence Angle	0 deg	90 deg	0 deg	90 deg	0 deg	90 deg
Rf=3Ω	0.0300	0.0504	0.1947	0.3526	4.1044	4.5936
Rf=30Ω	0.1654	1.9976	0.3839	0.3317	4.2969	2.7500

Table III. Error in % using Single-Line Algorithm

Simulation Parameters	Three Phase to Ground Fault					
Fault Location	0.25		0.45		0.75	
Incidence Angle	0 deg	90 deg	0 deg	90 deg	0 deg	90 deg
Rf=3Ω	0.0118	0.0604	0.0026	0.0483	0.1802	0.3590
Rf=30Ω	0.0066	0.0530	0.0166	0.0510	0.1671	0.3484

Table IV. Error in % using Parallel-Line Algorithm (Assumption 1)

Simulation Parameters	Three Phase to Ground Fault					
Fault Location	0.25		0.45		0.75	
Incidence Angle	0 deg	90 deg	0 deg	90 deg	0 deg	90 deg
Rf=3Ω	0.1403	0.1634	0.2013	0.2070	0.0334	0.2427
Rf=30Ω	0.1417	0.1637	0.2287	0.2284	0.0104	0.2273

Table V. Error in % using Single-Line Algorithm

Simulation Parameters	Phase B to Phase C Fault					
Fault Location	0.25		0.45		0.75	
Incidence Angle	0 deg	90 deg	0 deg	90 deg	0 deg	90 deg
Rf=3Ω	0.1206	0.0377	0.2208	0.0981	1.6423	0.9332
Rf=30Ω	6.7290	0.3739	1.7897	0.4265	9.0826	1.2763

Table VI. Error in % using Parallel-Line Algorithm (Assumption 1)

Simulation Parameters	Phase B to Phase C Fault					
Fault Location	0.25		0.45		0.75	
Incidence Angle	0 deg	90 deg	0 deg	90 deg	0 deg	90 deg
Rf=3Ω	0.0678	0.2070	0.6840	0.5732	2.0156	1.3242
Rf=30Ω	6.651	0.0890	1.6127	0.4466	8.9974	1.2127

Table VII. Error in % using Single-Line Algorithm

Simulation Parameters	Phase A to Phase B to Ground Fault					
Fault Location	0.25		0.45		0.75	
Incidence Angle	0 deg	90 deg	0 deg	90 deg	0 deg	90 deg
Rf=3Ω	0.4286	0.3633	0.3402	0.1785	0.2080	0.7854
Rf=30Ω	0.0802	0.1241	0.0844	0.0690	0.5870	0.6293

Table VIII. Error in % using Parallel-Line Algorithm (Assumption 1)

Simulation Parameters	Phase A to Phase B to Ground Fault					
Fault Location	0.25		0.45		0.75	
Incidence Angle	0 deg	90 deg	0 deg	90 deg	0 deg	90 deg
Rf=3Ω	0.1728	0.2232	0.1972	0.2214	0.6708	0.6482
Rf=30Ω	0.1912	0.2345	0.2479	0.2620	0.3148	0.3642

Table IX. Error in % using Parallel-Line Algorithm (Assumption 2)

Simulation Parameters	Phase A to Ground Fault					
Fault Location	0.25		0.45		0.75	
Incidence Angle	0 deg	90 deg	0 deg	90 deg	0 deg	90 deg
Rf=3Ω	-	-	-	-	0.2308	0.2888
Rf=30Ω	-	-	-	-	0.3683	1.5806

Table X. Error in % using Parallel-Line Algorithm (Assumption 2)

Simulation Parameters	Three Phase to Ground Fault					
Fault Location	0.25		0.45		0.75	
Incidence Angle	0 deg	90 deg	0 deg	90 deg	0 deg	90 deg
Rf=3Ω	-	-	-	-	0.0334	0.0838
Rf=30Ω	-	-	-	-	0.1099	0.0954

Table XI. Error in % using Parallel-Line Algorithm (Assumption 2)

Simulation Parameters	Phase B to Phase C					
Fault Location	0.25		0.45		0.75	
Incidence Angle	0 deg	90 deg	0 deg	90 deg	0 deg	90 deg
Rf=3Ω	-	-	-	-	0.7468	0.2501
Rf=30Ω	-	-	-	-	10.638	0.0920

Table XII. Error in % using Parallel-Line Algorithm (Assumption 2)

Simulation Parameters	Phase A to Phase B to Ground Fault					
Fault Location	0.25		0.45		0.75	
Incidence Angle	0 deg	90 deg	0 deg	90 deg	0 deg	90 deg
Rf=3Ω	-	-	-	-	0.0485	0.0404
Rf=30Ω	-	-	-	-	0.0773	0.0648

CONCLUSIONS

The paper presents a novel approach in solving the problem of the fault location on the transmission line having significant magnetic coupling with another transmission line. This approach uses synchronized samples of the end voltages and currents of the faulted line and the samples of currents from the magnetically coupled line. The exact fault location equation is derived for a short transmission line. This equation directly relates the samples taken and the location of the fault. The developed algorithm does not require any approximation, filtering of the sampled signals or the post fault steady state values. It can be applied to the faults having a time dependent resistance. Since phase voltages and currents are used, and the equations are valid for any type of the fault, there is no need to calculate phasor values or sequence voltages and currents. Such approach contributes to the computational simplicity and the execution speed of the algorithm. It offers the possibility to be used in on-line protection devices.

Evaluation of the algorithm using a real transmission line from Beaumont area was performed using EMTP generated tests. In most of the cases the calculation error was very low; less than 0.5 percent. However, in four cases the error was of the order of 2% or higher.

ACKNOWLEDGMENTS

The authors wish to acknowledge financial support for this project that came from the Graduate Studies and Research Institute, Lamar University, Beaumont. They are also thankful to Mr. Larry Dopson, Entergy Inc., for providing the data on a real transmission line and for his interest in this project.

REFERENCES

[1] R. E. Wilson, "Method and Uses of Precise Time in Power Systems," Transactions on Power Delivery, Vol. 7, No. 1, January 1992.

[2] IEEE Working Group Report, Power System Relaying Committee, "Synchronized Sampling and Phasor Measurements for Relaying and Control," IEEETransactions on Power Delievery, Vol. 9, 1994, pp 442-449

[3] Macrodyne, Inc. "Phasor Measurement Unit - Model 1690," Application/Performance Data Sheet, 1993.

[4] M. Kezunovic, J. Mrkic, and B. P. Perunicic, "Accurate Fault Location Using Synchronized Sampling at Two Ends of a Transmission Line." 11th Power System Computation Conference, Avignon, France, September 1993.

[5] M. Kezunovic, J. Mrkic, and B. Perunicic, "An Accurate Fault Location Algorithm Using Synchronized Sampling." Electric Power Systems Research Journal, Vol 29, 1994, pp 161-169.

[6] "Electromagnetic Transient Program (EMTP) Rule Book," EPRI EL-6421-I, Vol.1, 2, RP2149-4, June 1989.

[7] Electromagnetic Transient Program (EMTP) Workbook," EPRI EL-4651, Vol. 4, R. P. 2149-6, June 1989.

APPENDIX A

Consider a faulted three-phase system in Fig A-1. The fault point is denoted with F, and it is at the distance x from the line end S. Due to the fault occurrence at the point F, the transmission line is divided into two homogeneous parts, one from the sending end S to the fault point F, and the other one from the receiving end R to F. The relation between fault point F phase voltages and currents to line end S phase voltages and currents is:

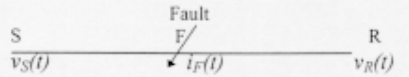

Figure A-1. One Line Representation of the 3-Phase Line

$$v_{FS} = L^v \{ v_S, i_S, x \} \quad \text{(A1)}$$
$$i_{FS} = L^i \{ v_S, i_S, x \} \quad \text{(A2)}$$

Similarly, the phase voltages and currents at the fault point F are related to the line end R phase voltages and currents as:

$$v_{FR} = L^v \{ v_R, i_R, d\text{-}x \} \quad \text{(A3)}$$
$$i_{FR} = L^i \{ v_R, i_R, d\text{-}x \} \quad \text{(A4)}$$

Because of the continuity of the voltages, (A1) and (A3) can be combined leading to:

$$v_{FS} = v_{FR}$$
$$L^v \{ v_S, i_S, x \} = L^v \{ v_R, i_R, d\text{-}x \} \quad \text{(A5)}$$

Linearity of operators L^v, L^i enables expressions (A5) to be rewritten as:

$$L^v \{ v_R\text{-}v_S, i_R\text{-}i_S, x, d \} = 0 \quad \text{(A6)}$$

The equation (A6) is the generic fault location equation presented in [4]. It relates the unknown distance x to the fault point F (from the line end S) and to the phase voltages and currents at both transmission line ends.

Derivation of Fault Location equations

The fault location equation for the single transmission line can be derived using the generic fault location equation of (A6) as follows:

$$v_{mR}(t) - v_{mS}(t) - d \sum_p [r_{mp} i_{pR}(t) + l_{mp}\, di_{pR}(t)/dt] + x [r_{mp} i_{pR}(t) + r_{mp} i_{pS}(t) + l_{mp}\, di_{pR}(t)/dt + l_{mp}\, di_{pS}(t)/dt] = 0 \quad \text{(A7)}$$

m = a, b, c p = a, b, c

Equation (A7) can be rewritten in discrete form as:

$$A_m(k) + B_m(k)\, x = 0 \quad \text{(A8)}$$

m = a, b, c and k = 1, ...N

Where $A_m(k)$ and $B_m(k)$ for m = a, b, c, and k = 1,....N are defined as:

$$A_m(k) = v_{mR}(k) - v_{mS}(k) - d\sum[(r_{mp} + (l_{mp}/\Delta t))\, i_{pR}(k) - (l_{mp}/\Delta t)\, i_{pR}(k\text{-}1)] \quad \text{(A9)}$$

$$B_m(k) = \{(r_{mp} + (l_{mp}/\Delta t))[i_{pR}(k) + i_{pS}(k)] - (l_{mp}/\Delta t)\, [i_{pR}(k\text{-}1) + i_{pS}(k\text{-}1)\} \quad \text{(A10)}$$

In the above equations, $v_{mS}(k)$, and $v_{mR}(k)$ are phase (m=a, b, c) voltage samples at the time instants $t = k\Delta t$ (k=1, ...N) at the line end S, and at the line end R, respectively. Similarly, $i_{mS}(k)$, and i_{mR} are phase currents at the line end S, and at the line end R. Here, Δt is the sampling step and N is the total number of samples. Thus x is determined using the lease square estimate for all the three phases together:

$$x = \frac{-[\sum_{m=a,b,c} \sum_{k=1}^{N} A_m(k)\; B_m(k)]}{[\sum_{m=a,b,c} \sum_{k=1}^{N} B^2_m(k)]} \quad \text{(A11)}$$

The expression (A11) is the explicit fault location equation.

Branislava Perunicic received her Dipl. Ing Degree in electrical engineering from University of Belgrade, Yugoslavia, and Candidate of Sciences Degree in automatic Control from the Institution of Automatics and Telemechanics of USSR Academy of Sciences, Moscow in 1960, and 1969 respectively.

From 1960 upto now she is with Energoinvest Company, Sarajevo, Yugoslavia. She joined the faculty of the University of Sarajevo, Yugoslavia, in 1964, where now she is a full professor. Currently, she is a professor in Electrical Engineering Department at Lamar University, Beaumont, Texas.

Asif Y. Jakwani (S'91) received his B.Sc. degree in electrical engineering from Lamar University, Beaumont, Texas in August 1993. Currently, he is a Graduate Research Assistant in Electrical and Computer Engineering Department at University of Texas at Austin. His areas of interest include power quality, power harmonics and modeling and simulation of power systems transients.

Mladen Kezunovic (S'77, M'80, SM'85) received his Dipl. Ing. Degree from University of Sarajevo, Yugoslavia, his M.Sc and PhD degrees from University of Kansas, all in electrical engineering in 1974, 1977 and 1980, respectively.

Dr. Kezunovic industrial experience is with Westinghouse Electric Corporation in the USA, and the Energoinvest Company in Yugoslavia. He was a Visiting Associate Professor at Washington State University during 1986-87 and Texas A&M University during 1987-89. He has been an Associate Professor at Texas A&M since 1992.